



Universiteit  
Leiden  
The Netherlands

## Hepatitis C virus intracellular host interactions

Liefhebber, J.M.P.

### Citation

Liefhebber, J. M. P. (2010, December 1). *Hepatitis C virus intracellular host interactions*. Retrieved from <https://hdl.handle.net/1887/16189>

Version: Corrected Publisher's Version

License: [Licence agreement concerning inclusion of doctoral thesis in the Institutional Repository of the University of Leiden](#)

Downloaded from: <https://hdl.handle.net/1887/16189>


**Note:** To cite this publication please use the final published version (if applicable).



**Characterisation of Hepatitis C  
virus NS3 modifications in  
the context of replication**

J Gen Virol. 2010 Apr; 91 (Pt4): 1013-8

Jolanda M.P. Liefhebber  
Paul J. Hensbergen  
André M. Deelder  
Willy J. M. Spaan  
Hans C. van Leeuwen



## Abstract

Post-translational modifications of viral proteins regulate various stages of infection and can even control cellular processes. With only 10 proteins Hepatitis C virus (HCV) can orchestrate its complete viral life cycle. The HCV non-structural protein 3 (NS3) has many functions. It has protease and helicase activity, interacts with several host cell proteins and plays a role in translation, replication and virus particle formation. Organisation of all these functions seems necessary and could be regulated by post-translational modifications. We therefore searched for modifications of the NS3 protein in the subgenomic HCV replicon. When performing a tag-capture approach coupled with two-dimensional gel electrophoresis analyses, we observed that isolated His6-NS3 yielded multiple spots. Individual protein spots were in-gel digested with trypsin and analysed by mass spectrometry. Differences observed between the individual peptide mass fingerprints suggested the presence of modified peptides and allowed us to identify N-terminal acetylation and an adaptive mutation of NS3 (Q1067R). Further analysis of other NS3 variants revealed phosphorylation of NS3.

## Introduction

Post-translational modifications (PTMs) like phosphorylation, prenylation, methylation and acetylation play an important role in protein activity, localisation and protein-protein interactions<sup>1,2</sup>. Not only eukaryotes use this mechanism to modulate the function(s) of their proteins. Especially viruses require PTMs because their genome is small and events like translation, replication, virus assembly and release all need to be well orchestrated<sup>3,4</sup>. The small 9,6 kb genome of Hepatitis C virus (HCV), a positive-stranded RNA virus, yields a single polyprotein, which after processing results in three structural proteins Core, E1 and E2, a peptide p7 and six non-structural proteins NS2, NS3, NS4a, NS4b, NS5a and NS5b. Together these 10 proteins coordinate the complete life cycle of HCV<sup>5</sup>. For some of these proteins it is known that they have a dual function involved in more than one process of the virus life cycle, requiring precise regulation<sup>6-9</sup>.

An apparent example of a multifunctional protein within the HCV genome is NS3, which contains protease and helicase activity<sup>10,11</sup>. The serine protease domain of NS3 is in the N-terminal one third of the protein. Together with NS4a it forms a stable complex, which cleaves the non-structural proteins, downstream of NS3<sup>12-14</sup>. Besides these cleavages, the NS3-4a protease is known to cleave MAVS/IPS-1/VISA/Cardif and TRIF, which affect signalling of the RIG-I and Toll-like receptor 3 pathways respectively, thereby abrogating the interferon response<sup>15</sup>.

Upon binding to NS4a the localisation of NS3 changes from cytosolic to endoplasmic reticulum (ER) membrane-associated, indicating that protein-protein interactions modulate its localisation<sup>16</sup>.

In addition to the protease activity of NS3 in the N-terminus, the C-terminus of NS3 can unwind RNA through ATP-ase and helicase activity<sup>11,17</sup>. RNA-unwinding activity seems to be modulated by other viral proteins like NS5b, the RNA-dependent RNA polymerase<sup>18,19</sup> and NS4a<sup>20</sup>. A fine balance between the concentration of NS5b, NS3 and RNA has been indicated to influence activity<sup>18</sup>. The helicase domain of NS3 can be post-translationally methylated at Arg1493 (polyprotein) by Protein Arginine Methyltransferase 1 (PMRT1)<sup>21</sup>. Non-methylated NS3 helicase can unwind dsDNA, however when the helicase domain of NS3 is methylated unwinding of dsDNA is inhibited<sup>22</sup>. This shows that methylation of the NS3 helicase domain can change its activity. The mechanism resulting in inhibition and the conditions for methylation

are still unclear, though proteins in the alpha interferon-induced signalling pathway have been implicated <sup>22</sup>.

Besides the interaction of NS3 with PMRT1, several other host-protein interactions with NS3 have been described, including PKA, PKC, TBK1 and p53, which are all proteins involved in cell signalling <sup>23-26</sup>. Recently a role in virus particle production has been suggested for NS3, by the identification of adaptation and compensatory mutations in NS3 using the infectious virus system <sup>27,28</sup>.

Taken together, the NS3 protein has various interaction partners and many functions which need to be regulated. Post-translational modifications could direct these processes. A first step towards understanding regulation is the identification of NS3 modifications. Besides methylation, which seems to regulate helicase activity and has been identified using over-expression of NS3, no other modifications are known. We therefore set up an assay to search for other NS3 modifications in the context of functional replication. In order to purify NS3 from the replicon, we introduced a His6-tag at the N-terminus of NS3 in the replicon RNA genome. After two-dimensional poly-acrylamide gel electrophoresis separation of purified NS3, at least 6 major protein spots corresponding to NS3 were observed. These spots point to several post-translational modifications of NS3. To identify post-translational modifications, we analysed spots by MALDI-ToF-ToF and LC-iontrap MS/MS and could reveal an N-terminal acetylation. In addition, an amino acid change in NS3, reported to enhance replication, was discovered. We furthermore show, by phosphate specific staining and phosphatase treatment, phosphorylation of NS3.

## Methods

### Plasmid Construction

To construct His6-tagged NS3-replicons, the sequence was amplified by PCR from pFK5.1Neo <sup>29</sup> using the specific primers GTTCGGACCGTCTAGACATCATCACCATCACCATGCGCCTATTACGGCCTACTCC and GAAGTCGACTGTCTGGGTGACAATG. The PCR product was digested with *RsrII* and *BsrGI* and ligated into pFK5.1Neo similarly digested with *RsrII* and *BsrGI*. Start codon and plasmid were restored by introducing PCR product derived from specific primers GCTAAGCTTCGTAATACGACTC and ATTCTAGACATGGTATTATCGT-

GTTTTTC, digested with *RsrII* - *XbaI* back into the construct. This resulted in the construction of a replicon containing a His6-tag at the N-terminus of NS3.

### Cell culture

Human hepatoma cell line Huh7 containing HCV replicons was grown in Dulbecco's Modified Eagle's Medium supplemented with Non-essential amino acids, L-glutamate, Penicillin, Streptavidin and Geneticin. Cells were subcultured using Trypsin.

### Purification of His6-NS3

Huh7 cells containing His6-tagged NS3 replicons were sub-cultured at least two days before cell lysis with Ureum buffer (8 M ureum, 300 mM NaCl, 1% NP40, 50 mM Tris pH 7.0 and 10 mM imidazole pH 7.0). Total lysate volume of each 15 cm culture dish was 2 ml. To get rid of cell debris, mainly genomic DNA, total cell lysates were subjected to centrifugation at 14.000  $\times$ g for 15 min at 4°C and supernatant was collected. Eighty  $\mu$ l of 50% Cobalt<sup>2+</sup>-beads (Clontech) in Ureum buffer was added to the supernatant of one dish and incubated for 2 h at 4°C under continuous rotation. Subsequently the beads were washed three times with Ureum buffer. His6-NS3 was eluted from the beads using Ureum buffer containing 190 mM imidazole. Proteins in the eluate were precipitated overnight at -20°C by adding 9 volumes of ethanol, followed by centrifugation at 14.000  $\times$ g for 1 h at 4°C. The protein pellet was either dissolved in Laemmli buffer or 2D-PAGE buffer (8 M ureum, 4% CHAPS, 15 mM Tris pH 8.5, 1% DTT, Brome phenol Blue (BPB) and 0.5% IPG-buffer (pH 3-10, GE-Healthcare).

### Two-dimensional poly-acrylamide gel electrophoresis (2D-PAGE)

Immobiline DryStrips pH 3-10, 13 cm (GE-Healthcare) were incubated for at least 6 h with 0.5% IPG-buffer in De-streak rehydration solution (GE-Healthcare), before starting isoelectric focusing of the sample. To apply the His6-NS3 samples (in 2D-PAGE buffer) onto the strip we used cup-loading at the basic end of the strip. Isoelectric focusing was performed on an Ettan IPGphor™ 3 Isoelectric Focusing System running the following program: 3 h at 150 V, 3 h at 300 V, gradually to 1000 V in 6 h, gradually to 8000 V in 1 h and 8000 V for 2 h. After first dimension separation the strip was equilibrated to SDS-PAGE conditions with two consecutive 15 min incubation steps with Equilibration buffer (6 M ureum, 50 mM Tris (pH 8.8), 30% glycerol and 4% SDS), which contained in the first step 2% DTT and in the

second 2.5% iodoacetamide and BPB. Subsequently the strips were applied to SDS-PAGE gels and covered with agarose. Following second dimension separation, gels were subjected to western blotting, silver staining, or ProQ diamond staining.

### **Western blotting**

After separation on SDS-PAGE gels, proteins were transferred to PVDF membranes (Hybond P, GE-Healthcare) using a Semi-Dry blot apparatus (Biorad). Membrane blocking and antibody incubations were performed using 0.5% Tween-20, 5% non-fat, dry milk (Campina) in PBS. Monoclonal anti-NS3 was obtained from Novo Castra. Goat-anti-mouse (DAKO) conjugated to horseradish peroxidase together with enzyme-catalysed chemoluminescence (ECL+, GE-Healthcare) and Fuji Super RX medical X-ray film or Typhoon imager (GE-Healthcare) were used to visualise the signal.

### **Silver staining**

SDS-PAGE gels were incubated in 50% ethanol, 12% acetic acid and washed with 50% ethanol. Sensitisation was performed using sensitise solution (1.5 mM sodiumthiosulfate) for 30 min, which was followed by washing with H<sub>2</sub>O. Subsequently Silver solution (12 mM silvernitrate, 0.075% formaldehyde) was added for 30 min. After rinsing the SDS-PAGE gel in H<sub>2</sub>O, it was stained with Develop solution (2.5% sensitise solution, 0.57 M sodiumcarbonate, 0.05% formaldehyde) until desired staining was reached. The staining reaction was stopped with 50% methanol, 12% acetic acid.

### **Phosphatase treatment**

Purified His6-NS3 eluted from the Cobalt<sup>2+</sup>-beads was diluted to 1 M Urea using PBS (154 mM NaCl, 1.4 mM Phosphate, pH 7.5). Subsequently the phosphatase treatment was performed in the presence of 5 mM Tris pH 8.0 and 1 mM MgCl<sub>2</sub> with 1 unit Shrimp Alkaline Phosphatase (SAP) (USB) per 64 µl. Both the phosphatase-treated and the control sample, to which no SAP was added, were incubated at 37°C for 1h. After that, the samples were concentrated using ethanol precipitation as described above and the protein pellets were dissolved in 2D-PAGE buffer.

### **ProQ diamond staining**

SDS-PAGE gels were fixed in 50% methanol, 10% acetic acid, washed with H<sub>2</sub>O and stained for 1.5 h with Pro-Q Diamond phosphoprotein gel stain (Invitrogen). Then destaining was performed using 20% acetonitrile, 50 mM sodium acetate, pH

4.0 for a total time of 1.5 h. Until imaging, the gel was stored in H<sub>2</sub>O. To visualise the ProQ diamond signal we used the Typhoon imager (excitation 532nm; emission filter 560nm; GE Healthcare).

### **In-gel tryptic digestion**

Protein spots were excised, cut into small pieces and washed with 25 mM NH<sub>4</sub>HCO<sub>3</sub> followed by dehydration with 100% acetonitrile (ACN) for 10 min. For reduction and alkylation, dried gel particles were first incubated with 10 mM dithiothreitol for 30 min at 56 °C. Following dehydration with ACN, gel plugs were subsequently incubated in 55 mM iodoacetamide for 20 min at room temperature. After washing with 25 mM NH<sub>4</sub>HCO<sub>3</sub> and dehydration with 100% ACN, the gel particles were completely dried in a centrifugal vacuum concentrator (Eppendorf, Hamburg, Germany). Dried gel particles were re-swollen for 15 min on ice by addition of 10-15 µl of a trypsin solution (12.5 ng/µl in 25 mM NH<sub>4</sub>HCO<sub>3</sub>, sequencing grade modified trypsin, Promega, Madison, WI). Following this, 25-35 µl of 25 mM NH<sub>4</sub>HCO<sub>3</sub> was added and samples were kept on ice for an additional 30 min. Tryptic digestion was subsequently performed overnight at 37 °C. Following tryptic digestion, the overlaying digestion-solution was collected (extract 1). Two additional rounds of extraction with 20 µl 0.1% TFA were used to extract peptides from the gel plugs and these were pooled with extract 1.

### **MALDI-ToF MS**

For MALDI-ToF, tryptic digestions were desalted using C<sub>18</sub> ZipTips (Millipore) according to the manufacturer's instructions. Peptides were eluted using approx. 1 µl of 0.33 mg/ml alpha-cyano-4-hydroxycinnamic in acetone:ethanol 1:3 and spotted directly on a 600 µm AnchorChip MALDI target plate (Bruker Daltonics, Bremen, Germany) and allowed to dry. MALDI-ToF(-ToF) analyses were performed on an Ultraflex II time-of-flight mass spectrometer (Bruker Daltonics, Bremen, Germany) controlled by the Flexcontrol 2.0 software package. Spectra were recorded in the positive ion reflectron mode at a laser frequency of 50 Hz. For MS/MS analysis, precursors were accelerated and selected in a time ion gate after which laser-decomposed fragments were further accelerated in the LIFT cell and their *m/z* were analysed after passing the ion reflectron.

### **Nano-LC-iontrap MS**

Tryptic digests were separated on a C<sub>18</sub> pepmap100 column (75 µm I.D., 15 cm

long; Dionex, Amsterdam, The Netherlands) coupled to an electrospray ionisation (ESI)-iontrap mass spectrometer (HCTultra, Bruker Daltonics, Bremen, Germany). The gradient profile started with 100% solvent A (20% ACN/0.1% formic acid) for 10 min. This was followed by a 20 min linear gradient from 20% solvent B (95% ACN/0.1% formic acid) up to 60% solvent B. The system remained at 60% solvent B for 25 min followed by a second linear gradient up to 90% solvent B in 10 min. After 30 min at 90%, solvent B the gradient was changed to 0% solvent B. The flow rate was maintained at 200 nL/min during the entire run. Eluting peptides were analysed in data dependent MS/MS mode over a 400–1600  $m/z$  range. The five most abundant ions in each MS spectrum were selected for MS/MS analysis by collision-induced dissociation, using helium as collision gas. Mass spectra were evaluated using the DataAnalysis 3.1 software package (Bruker Daltonics, Bremen, Germany).

## Results

### Purification of NS3 from HCV selectable replicons

Besides methylation of the helicase domain of NS3 no other post-translational modifications (PTMs) of NS3 have been reported. Our objective was to identify novel NS3 PTMs in the context of actively replicating HCV RNA. For this purpose, we introduced a His6-tag to NS3 in the HCV replicon (Con1 genotype 1b containing NS3 to NS5b, see Methods), providing an unlimited source of HCV proteins actively replicating HCV RNA (Supplemental figure 1). Addition of the His6-tag did not influence replicon colony formation efficiency (Supplemental figure 1). RT-PCR sequencing of the replicon cell-line furthermore confirmed that the six histidines remained unchanged at passage 30 at which stage our experiments were conducted (Supplemental figure 1). In addition, lysates of the His6-NS3 replicon cell line show that the extra tag resulted in a slightly higher molecular weight compared to the control cell line (Fig. 1A, lanes 1 and 2). Based on western blot, using NS3 antibody (NCL-HCV-NS3, Novagen) similar amounts of NS3 are expressed by both cell lines (Fig. 1A).

An additional advantage of a His6-tag is that it allows for affinity purification under denaturing conditions. Hence, to maximise yields of purified NS3, an ureum/NP40-based buffer was used to lyse the cells and, following centrifugation, the His6-NS3 was purified from the supernatant using Cobalt<sup>2+</sup> beads (See Methods). Figure 1 shows

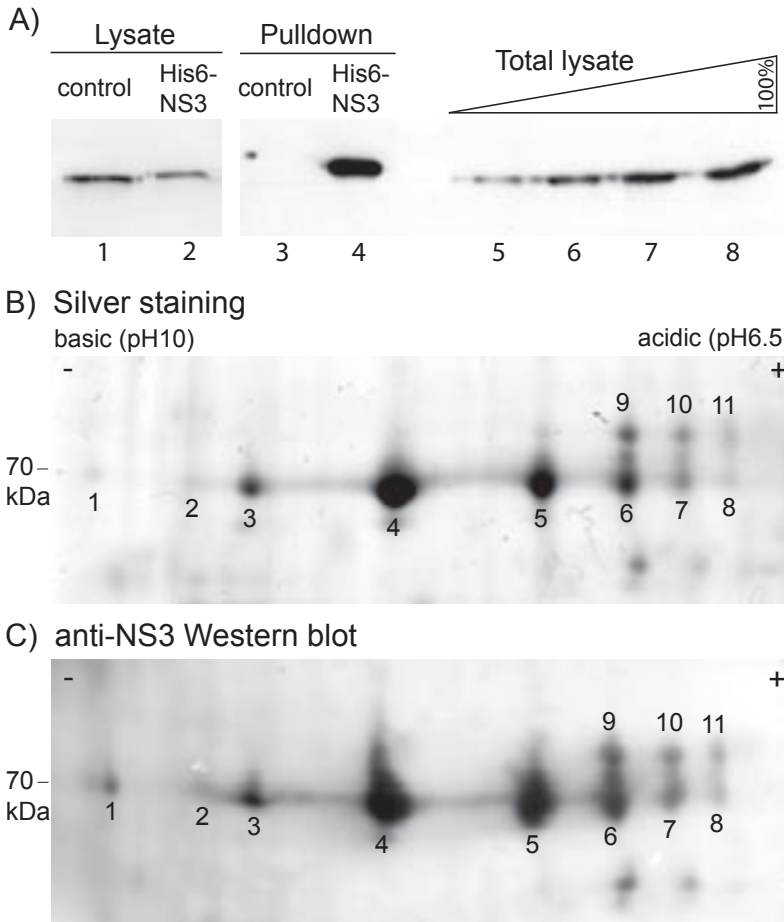
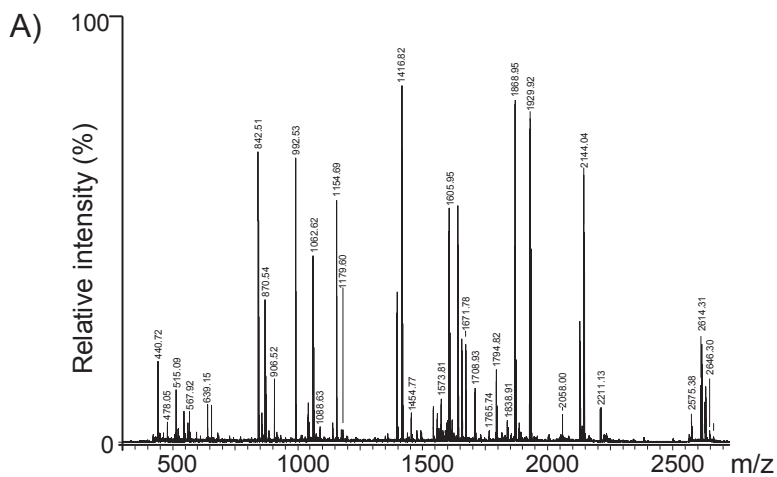


**Figure 1 - Affinity purification and 2D-PAGE analysis of NS3 isoforms from Huh7 replicon cell line**

**A.** Lysates of Huh7 replicon cells containing non-tagged NS3 (Control, lane 1) or His6-tagged NS3 (His6-NS3, lane 2), standardised to protein concentration using Bradford reagent (Biorad), were separated by SDS-PAGE, followed by western blot analysis with anti-NS3. These lysates were subjected to affinity purification under denaturing conditions, using Cobalt<sup>2+</sup>-beads (See Methods for further details). Lanes 3 and 4 represent (His6-)NS3 bound to the beads from control or His6-NS3 cell lines, respectively. Lanes 5 to 8 contain increasing volumes of total cell lysate from His6-NS3 cells, with 100% corresponding to the total amount of His6-NS3 used for pulldown.

Isolated His6-NS3 was separated on 2D-PAGE, followed by either silver staining (**B**) or western blotting using NS3-antibody (**C**). Each His6-NS3 spot is labelled with a number. Basic and acidic indicate where the negative and positive pole are positioned.



B)

1	MSRHHHHHHA	PITAYSQQTR	GLLGCIIITSL	TGRDRNQVEG	EVQVSVSTATQ
51	SFLATCVNGV	CWTVYHGAGS	KTLAGPKGPI	TQMYTNVDQD	LVGWQAPPGA
101	RSLTPTCCGS	SDLYLVTRHA	DVIPVRRRGD	SRGSLLSPRP	VSYLKGSSGG
151	PLLCPSGHAV	GIFRAAVCTR	GVAKAVDFVP	VESMGTTRS	PVFTDSSPP
201	AVPQTFQVAH	LHAPTGSQKS	TKVPAAYAAQ	GKVLVNLNPS	VAATLGFQAY
251	MSKAHGIDPN	IRIGVRTITT	GAPITYSTYG	KFLADGGCSG	GAYDIIICDE
301	CHSTDSTTIL	GIGTVLDQAE	TAGARLVVLA	TATPPGSVTV	PHPNIEEVAL
351	SSTGEIPFYG	KAIPIETIKG	GRHLIFCHSK	KKCELAAKL	SGLGLNAVAY
401	YRGLDVSVIP	TSGDVIVVAT	DALMTGFTGD	FDSVIDCNTC	VTQTVDVDFSLD
451	PTFTIETTTV	PQDAVRSQR	RGRTGRGRMG	IYRFVTPGER	PSGMFDSVSL
501	CECYDAGCAW	YELTPAETSV	RLRAYLNTPG	LPVCQDHLEF	WESVFTGLTH
551	IDAHFLSQTK	QAGDNFPYLV	AYQATVCARA	QAPPPSWDQM	WKCLIRLKP
601	LHGPTPLLYR	LGAVQNEVTT	THPI TKYIMA	CMSADLEVVT	

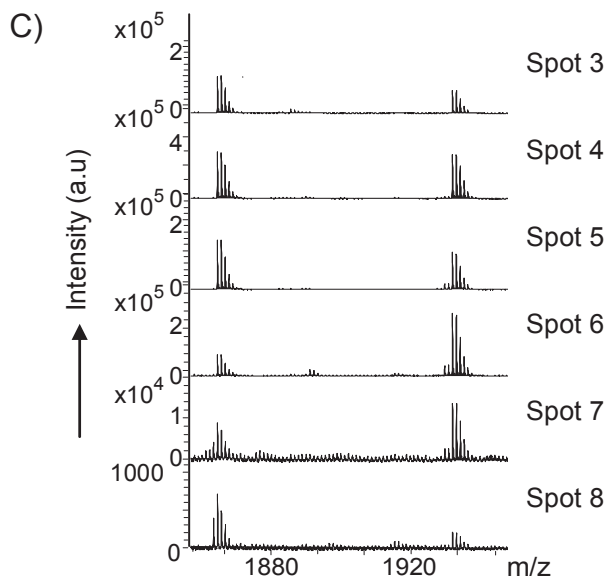


**Figure 2 - MALDI-ToF analysis of affinity purified and 2D-PAGE separated NS3-isoforms**

His6-tagged NS3 was affinity purified and separated using 2D-PAGE. Six individual proteins spots (3-8, Fig.1B) were digested with trypsin and analysed by MALDI-ToF MS. **A.** MALDI-ToF spectrum showing individual tryptic peptides from NS3. **B.** Primary sequence of His6-tagged NS3 with the sequence coverage obtained with MALDI-ToF MS in bold. **C.** Comparison of MALDI-ToF spectra showing two of the most abundant NS3 tryptic peptides (see A) in all the six protein spots.

specific pulldown of NS3, only when it is His6-tagged (compare lane 3 (control) and lane 4 (His6-NS3)). When relating the amount of purified His6-NS3 (lane 4) to the total amount of His6-NS3 in the lysate (lane 8), it is apparent that almost all the NS3 is pulled down under these purification conditions. This high yield makes it likely that all NS3 isoforms, if present, are isolated using this method.

**2D-PAGE separation of NS3 isoforms**

Protein isoforms may arise from PTMs, which introduce a variation in the molecular mass and/or charge of a protein. These isoforms can be efficiently separated on the basis of isoelectric point and molecular weight in 2D-PAGE (two-dimensional polyacrylamide gel electrophoresis). To examine possible isoforms of NS3, we analysed purified His6-NS3 using this approach. His6-NS3 was visualised by means of silver staining (Fig.1B) or western blot using NS3 specific antibodies (Fig.1C). With both techniques, at least 11 NS3 protein spots were resolved, with a pI ranging from approximately 7 to 9 and with an apparent molecular mass around 70 kDa. Lower molecular weight products were considered to be NS3 breakdown products. The split of NS3 into multiple pI variants indicate several NS3 protein modifications in the context of replication.

**Tryptic digestion and MALDI-ToF analysis of individual NS3 spots**

To unravel possible PTMs, responsible for the appearance of multiple spots of His6-NS3 after 2D-PAGE separation, tryptic digestion followed by mass spectrometric analysis was performed on spots 3 to 8. As an example, the MALDI-ToF spectrum of spot 5 is shown in Figure 2A. Additionally, samples were measured in a higher mass range (between  $m/z$  3000-6000, data not shown). In total, peptides assigned to HCV NS3 add up to 60% coverage (Fig.2B, bold sequence). Although the sequence coverage was much lower in the digests of spots 7 and 8, NS3 specific peptides were also observed in these spectra (Fig.2C), confirming the results from the western blot

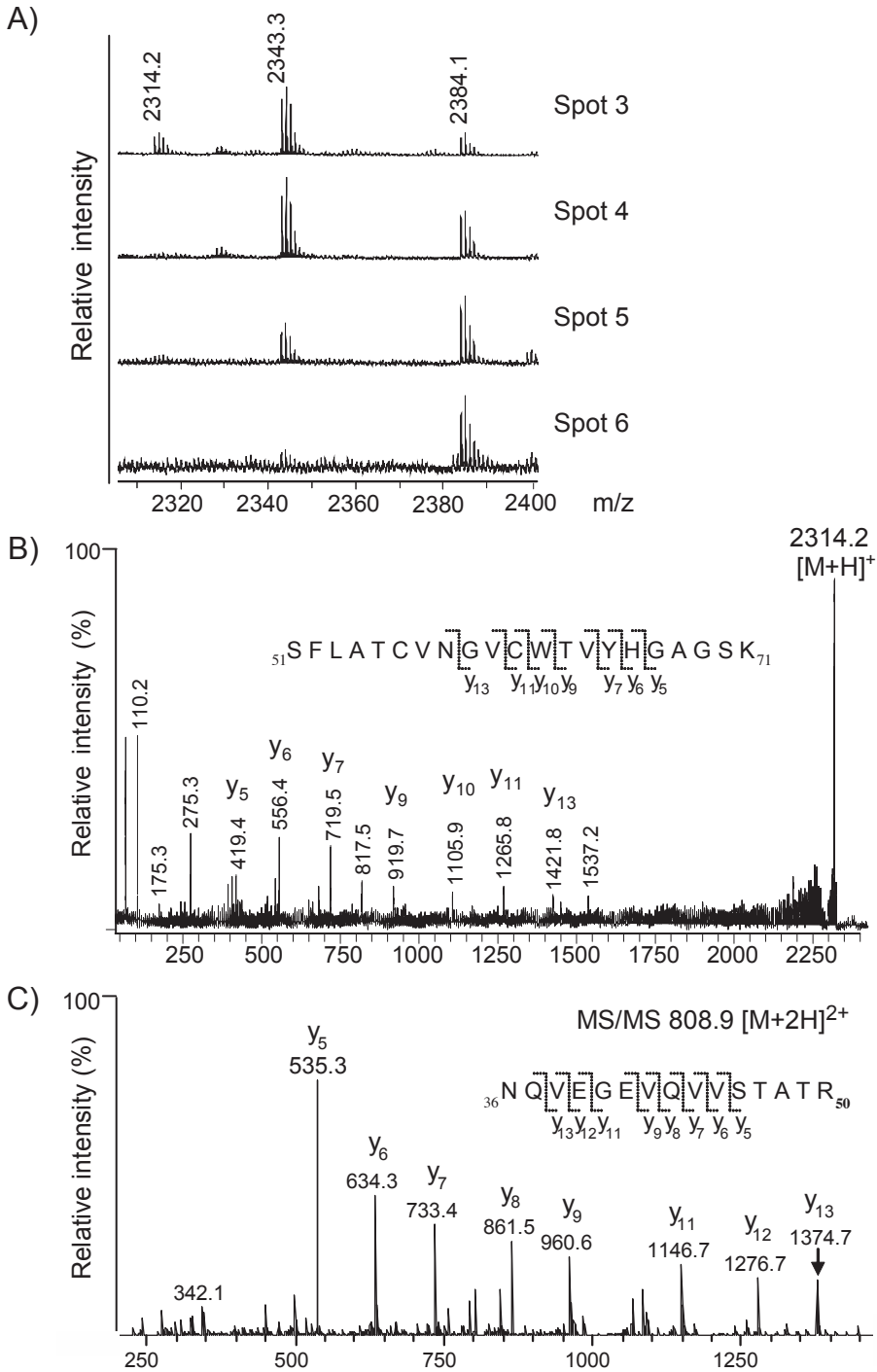


**Figure 3 - Mass spectrometric characterization of NS3 mutation and post-translational modification**

**A.** Comparison of MALDI-ToF spectra from NS3 isoforms in spots 3-6 (Fig.1B) The unique presence of a peptide at  $m/z$  2314.2 in the tryptic digest of spot 3 and absence of the tryptic peptide at  $m/z$  2343.3 in spot 6 are shown. MALDI-ToF-ToF revealed that the peptide at  $m/z$  2343.3 corresponds to the acetylated N-terminal tryptic peptide of NS3, Ac-SRHHHHHHAPITAYSQQTR (data not shown)

**B.** MALDI-ToF-ToF analysis of the peptide at  $m/z$  2314.2 showing that it matches with the peptide SFLATCVNGVCWTVYHGAGSK, corresponding to amino acid 51-71 in NS3 (Fig.2B). **C.** Identification of a peptide in the LC-MS run from the digest of protein spot 3, confirming Gln to Arg substitution at position 50 within NS3.

(Fig.1C). Since we observed similar intensities and comparable sequence coverages for the spots 3-6 (Fig.2C), these spectra were used for side-by-side comparison.

**Identification of a Gln to Arg mutation in NS3**

In the MALDI-ToF MS spectrum of spot 3, a peptide at  $m/z$  2314.2 was observed, which was absent in the other spectra (Fig.3A). This mass could not be matched to an *in silico* tryptic peptide of NS3. MALDI-ToF-ToF analysis revealed that this ion corresponds to the peptide SFLATCVNGVCWTVYHGAGSK (aa 51-71, Fig.3B). This was unexpected because at position 50 within NS3 there is no tryptic cleavage site (Arg or Lys). We therefore speculated that NS3 corresponding to this spot was mutated at position 50. Indeed, using LC-MS, a peptide was observed with an Arg at position 50 (NQVEGVQVVSTATR (Fig.3C). Altogether, this revealed a Gln to Arg mutation in NS3 at position 50, corresponding to position 1067 of the polyprotein (HCV type 1b genome Con-1, AJ238799), which is likely to alter the isoelectric point of NS3.

**Molecular mass based identification of HCV NS3 N-terminal acetylation.**

During further analysis of the spots by MALDI-ToF a unique peptide at  $m/z$  2343.3 was observed in spots 3, 4 and 5, which was absent in spot 6 (Fig.3A). This mass could not be assigned to any *in silico* tryptic peptide belonging to NS3. MALDI-ToF-ToF and manual inspection of the spectrum revealed a series of His residues in this peptide (data not shown). This indicates that the peptide corresponds to the N-terminus of NS3 and suggests that an N-terminal modification can explain these results. Indeed N-terminal acetylation (including removal of the Met) would

generate a  $m/z$  of 2343.3 (Acetyl-SRHHHHHHAPITAYSQQTR) corresponding to the observed mass and also would explain the MALDI-ToF-ToF fragmentation pattern (data not shown). This modification, which occurs on approximately 85% of all eukaryotic proteins<sup>30</sup>, could therefore at least explain some of the different spots we observed. It should be noted that normally the N-terminal end of NS3 is generated by (auto-) proteolytic cleavage of the HCV polyprotein and that the initiator methionine is added for construction in the HCV replicon<sup>31</sup>.

Additional comparison of the MALDI-ToF spectra derived from the separate spots yielded no qualitative differences that could be explained by modifications. In conclusion, using this mass spectrometry based approach, we elucidated one modification and a mutation, but still lack an explanation for the other different isoforms observed.

### HCV NS3 is phosphorylated

One of the most common post-translational modifications of proteins is phosphorylation (estimated one third of all cellular proteins<sup>32</sup>), which leads to a change of the net charge of proteins and thus the migration behaviour during 2D-PAGE. Consequently, comparison of 2D-gel spot patterns before and after treatment of the sample with a

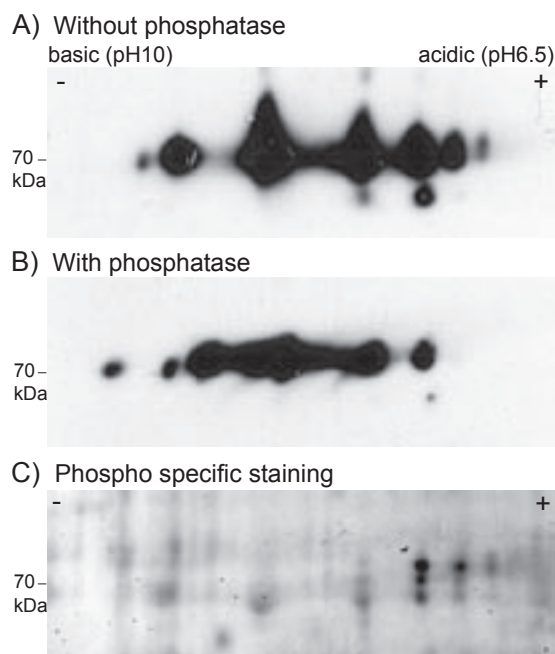


**Figure 4 - NS3 phosphorylation**

Purified His6-NS3 from Huh7 replicons was incubated without (**A**, **C**) or with alkaline phosphatase (**B**) at 37°C for 1 h. The samples were then concentrated, followed by separation on isoelectric point and molecular weight. Subsequently western blot detection was performed using anti-NS3 (**A**, **B**). Alternatively, the gel was directly stained with a phospho-specific stain (See Methods) (**C**). The negative and positive pole position are indicated with basic and acidic, respectively.

phosphatase can be utilised to assess the phosphorylation state of a protein<sup>33</sup>.

Therefore, phosphatase treated and untreated His6-NS3 samples were analysed by 2D-PAGE and stained with NS3 antiserum. In the untreated sample, we detected several spots in a similar pattern as shown before (Fig.4A). Upon treatment with phosphatase, the two most acidic spots disappeared and one extra spot appeared at the alkaline (basic) side of the gel (compare Fig.4A and B). This shift of spots towards the basic pole, after removing negatively charged phosphate group, clearly indicates phosphorylation of His6-NS3. Distinct spots resembling spots 9, 10 and 11 in Figure 1C were not detected in these experiments. This might be due to the long phosphatase procedure before separation in the two-dimensional gel electrophoresis (see Methods).

To further corroborate these results, we stained the 2D-PAGE gels directly with proQ diamond, a dye that selectively stains phosphorylated proteins in polyacrylamide gels (Fig.4C). The phospho-specific stain mainly coloured the acidic spots, which are the low abundant isoforms of NS3. Conversely, highly abundant NS3 isoforms were hardly stained. This is in accordance with the phosphatase treatment experiment, as the most acidic spots are lost after addition of phosphatase.

Taken together, the phosphospecific staining and the de-phosphorylation assay strongly suggest phosphorylation of NS3.

## Discussion

Identification of NS3 modifications in the context of self-replicating HCV RNA is complicated, given that only low amounts of protein are available and a combination of processes can influence the modification states of NS3. For that reason we designed an isolation method to purify NS3 from replicon cells. A His6-tag was added to the N-terminus of NS3 in this system that comprises HCV proteins NS3 to NS5b. With this approach, high amounts of NS3 can be isolated (Fig.1A) and is thus likely to include all NS3 isoforms. Since modifications can induce changes in the isoelectric point (pI) and molecular weight of proteins, NS3 variants were visualised by two-dimensional gel electrophoresis (2D-PAGE). Purified NS3 was found to show multiple pI variants (Fig.1B and C), indicating several NS3 protein modifications in the context of replication. We uncovered protein modifications for some NS3 isoforms using various approaches.

Using mass spectrometry, we analysed four NS3 spots (spots 3-6) for modifications. Comparison of MALDI-ToF spectra from spots 3, 4 and 5 with spot 6 resulted in the identification of N-terminal acetylation of His6-NS3 (Fig.3A,  $m/z$  2343.3). N-terminal acetylation is the most common covalent modification of eukaryotic proteins<sup>30</sup> and can affect protein-protein interactions, activity or stability of proteins<sup>34-36</sup>. Viral proteins can also be acetylated at their N-terminus, such as mature Core protein from HCV and Gag protein from L-A double-stranded RNA virus<sup>37, 38</sup>. In the latter virus acetylation affects viral assembly<sup>38</sup>. Since we use the HCV replicon system acetylation might be the result of the introduced starting methionine used in this construct. However, we cannot exclude N-terminal acetylation on proteolytically processed NS3 derived from the polyprotein.

Another change we observed was a Gln to Arg mutation at position 50 (corresponding to 1067 in the polyprotein), which would add a significant charge difference to the NS3 protein (pI 7.5 versus 7.8). This mutated arginine residue introduced an extra trypsin cleavage site resulting in two peptides (NQVEGVQVVSTATR at  $m/z$  808.9  $[M+2H]^{2+}$  and SFLATCVNGVCWTVYHGAGSK at  $m/z$  2314.2  $[M+H]^+$ ), respectively) in spot 3 of NS3 (Fig.3). This Q1067R is located close to the active site of the NS3 protease<sup>39</sup>. An identical mutation at this position was described for a HCV genotype 1a replicon<sup>40</sup>. Interestingly, this mutation was shown to compensate for a negative effect located in the proximal NS3 protease region of the HCV genotype 1a and found to enhance the replication capacity of the viral RNA<sup>40</sup>. Surprisingly, we now observe this compensating mutation at the protein level in the Con1 HCV genotype 1b, which is normally not down modulated and does not accumulate mutations at this position.

Protein phosphorylation is an important regulator of diverse intracellular processes. HCV NS5a is a phosphoprotein, involved in replication and virus particle formation. In both processes the phosphorylation status of NS5a was shown to be critical<sup>8, 41-43</sup>. The multifunctional protein NS3 might be regulated in a similar way. Since we observed a train of spots, which might indicate phosphorylation, we investigated this possibility for NS3. Both treatment with phosphatase and specific staining of phosphate groups by ProQ diamond illustrate phosphorylation of NS3 (Fig.4). Multiple phosphorylation sites are suggested within NS3 using the phosphorylation prediction program NetPhos 2.0, i.e. 17 serine-, 13 threonine- and 4 tyrosine-

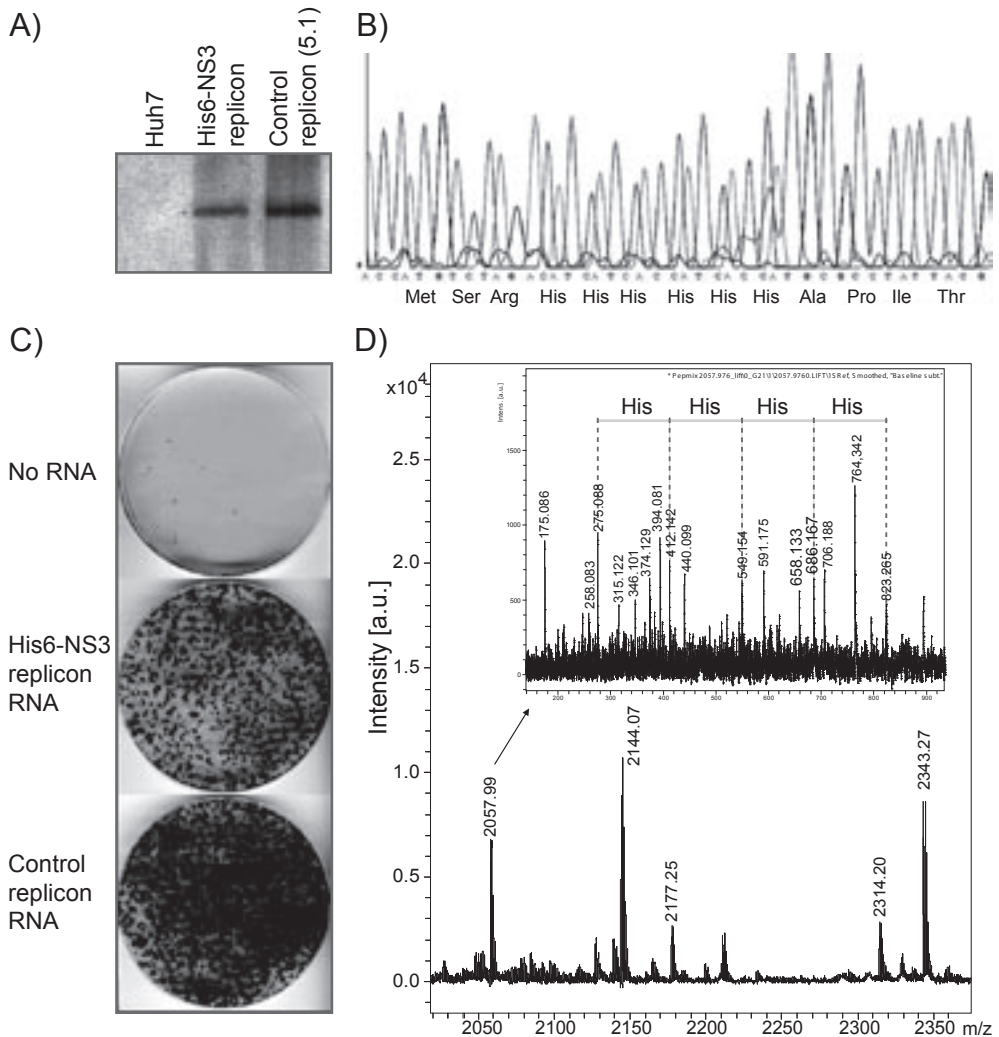
phosphorylation sites. As illustrated in Figure 4 phosphorylated NS3 protein is low abundant, therefore concentration of phosphorylated peptides was necessary to try to identify the phosphorylated amino acid in NS3. Phosphorylated peptides, generated from a pool of NS3 isoforms, were enriched using TiO<sub>2</sub>-beads prior to analysis by mass spectrometry. However, using this approach no phosphorylated peptides could be identified. As illustrated in Figure 3 phosphorylated NS3 protein is low abundant. Additionally lower signal intensities are often observed for phosphopeptides, possibly due to low ionisation efficiency<sup>44</sup>. Moreover, the phosphorylation site might be located within a tryptic peptide that is not well suited for our standard mass spectrometric analysis (Fig.2B). Usually tryptic digestions are measured in the mass range of 500 to 3500 Da. When only peptides between 500 and 3500 Da from the in-silico digest of His6-NS3 were taken into account, we observed coverage around 92%. Altogether, this might explain the difficulty to identify the site of phosphorylation.

pI heterogeneity of a protein can be generated by PTMs, chemical reactions like deamination<sup>45</sup>, or it could be due to conformational isomers of a protein<sup>46</sup>. All result in multiple isoforms observed in 2D-PAGE. In contrast a PTM that does not affect the pI of proteins is methylation<sup>47</sup>. Methylation was described to take place on amino acid 1493 and/or 1490 of NS3 (Fig.2B, aa 473 and 475)<sup>21</sup>. In our experiment, we were not able to detect specific peaks in this region, since digestion with trypsin in the area of NS3 methylation generates very small peptides (5 amino acids), which are difficult to assign specifically to NS3.

Taken together we identified modifications of His6-NS3 in the context of self-replicating HCV RNA, such as N-terminal acetylation, a Q1067R point mutation and phosphorylation. Resolving the precise sites of phosphorylation and determining their function will be the next challenging step. Generation of replicons with mutations in the predicted phosphorylation sites, in total around 34 sites, followed by 2D-PAGE analysis could result in identification of specific phosphorylation sites, which might help our understanding of the orchestration of the HCV life cycle.

## Acknowledgements

We thank Ms. Irina Dragan and Ms. Janine Rattke for expert technical assistance.



### Supplemental figure 1 - Analysis of the His6-NS3 replicon cell line.

- A.** [ $^3\text{H}$ ] uridine labeling of total RNA isolated from  $1 \times 10^6$  cells incubated for 12 hours in the presence of  $50 \mu\text{Ci}$  of [ $^3\text{H}$ ] uridine and  $5 \text{mg/ml}$  Actinomycin D.
- B.** Isolated RNA from the His6-NS3 replicon was subjected to sequence analysis after reverse transcriptase and PCR amplification of the 5' region of NS3.
- C.** Coomassie stained culture dish 3-weeks after electroporation of Huh-7 cells with no (top) or  $10 \text{ ng}$  of *in vitro* transcribed His6-NS3 tagged replicon RNA (middle) or untagged control replicon RNA in the presence of  $500 \mu\text{g/ml}$  G418 (bottom).
- D.** MALDI-ToF and MALDI-ToF-ToF of  $2058 \text{ [M+H]}^+$  corresponding to N-terminal tryptic peptide of NS3 showing the presence of the consecutive histidines.

## References

1. **Mann M, Jensen ON** Proteomic analysis of post-translational modifications. *Nat Biotechnol* 2003;21:255-61.
2. **Schweppe RE, Haydon CE, Lewis TS, Resing KA, Ahn NG** The characterization of protein post-translational modifications by mass spectrometry. *Acc Chem Res* 2003;36:453-61.
3. **Bartenschlager R, Frese M, Pietschmann T** Novel insights into hepatitis C virus replication and persistence. *Adv Virus Res* 2004;63:71-180.
4. **Jakubiec A, Jupin I** Regulation of positive-strand RNA virus replication: the emerging role of phosphorylation. *Virus Res* 2007;129:73-9.
5. **Moradpour D, Penin F, Rice CM** Replication of hepatitis C virus. *Nat Rev Microbiol* 2007;5:453-63.
6. **Kim SJ, Kim JH, Kim YG, Lim HS, Oh JW** Protein kinase C-related kinase 2 regulates hepatitis C virus RNA polymerase function by phosphorylation. *J Biol Chem* 2004;279:50031-41.
7. **Lindenbach BD, Pragai BM, Montserret R, Beran RK, Pyle AM, Penin F, Rice CM** The C terminus of hepatitis C virus NS4A encodes an electrostatic switch that regulates NS5A hyperphosphorylation and viral replication. *J Virol* 2007;81:8905-18.
8. **Tellinghuisen TL, Foss KL, Treadaway J** Regulation of hepatitis C virion production via phosphorylation of the NS5A protein. *PLoS Pathog* 2008;4:e1000032.
9. **Yu GY, Lee KJ, Gao L, Lai MM** Palmitoylation and polymerization of hepatitis C virus NS4B protein. *J Virol* 2006;80:6013-23.
10. **Bartenschlager R** The NS3/4A proteinase of the hepatitis C virus: unravelling structure and function of an unusual enzyme and a prime target for antiviral therapy. *J Viral Hepat* 1999;6:165-81.
11. **Kim DW, Gwack Y, Han JH, Choe J** C-terminal domain of the hepatitis C virus NS3 protein contains an RNA helicase activity. *Biochem Biophys Res Commun* 1995;215:160-6.
12. **Bartenschlager R, Lohmann V, Wilkinson T, Koch JO** Complex formation between the NS3 serine-type proteinase of the hepatitis C virus and NS4A and its importance for polyprotein maturation. *J Virol* 1995;69:7519-28.
13. **Failla C, Tomei L, De FR** Both NS3 and NS4A are required for proteolytic processing of hepatitis C virus nonstructural proteins. *J Virol* 1994;68:3753-60.
14. **Tanji Y, Hijikata M, Satoh S, Kaneko T, Shimotohno K** Hepatitis C virus-encoded nonstructural protein NS4A has versatile functions in viral protein processing. *J Virol* 1995;69:1575-81.
15. **Meurs EF, Breiman A** The interferon inducing pathways and the hepatitis C virus. *World J Gastroenterol* 2007;13:2446-54.
16. **Wolk B, Sansonno D, Krausslich HG, Dammacco F, Rice CM, Blum HE, Moradpour D** Subcellular localisation, stability, and trans-cleavage competence of the hepatitis C virus NS3-NS4A complex expressed in tetracycline-regulated cell lines. *J Virol* 2000;74:2293-304.
17. **Suzich JA, Tamura JK, Palmer-Hill F, Warrenner P, Grakoui A, Rice CM, Feinstone SM, Collett MS** Hepatitis C virus NS3 protein polynucleotide-stimulated nucleoside triphosphatase and comparison with the related pestivirus and flavivirus enzymes. *J Virol* 1993;67:6152-8.
18. **Jennings TA, Chen Y, Sikora D, Harrison MK, Sikora B, Huang L, Jankowsky E, Fairman ME, Cameron CE, Raney KD** RNA unwinding activity of the hepatitis C virus NS3 helicase is modulated by the NS5B polymerase. *Biochemistry* 2008;47:1126-35.
19. **Zhang C, Cai Z, Kim YC, Kumar R, Yuan F, Shi PY, Kao C, Luo G** Stimulation of hepatitis C virus (HCV) nonstructural protein 3 (NS3) helicase activity by the NS3 protease domain and by HCV RNA-dependent RNA polymerase. *J Virol* 2005;79:8687-97.
20. **Gallinari P, Paolini C, Brennan D, Nardi C, Steinkuhler C, De FR** Modulation of hepatitis C virus NS3 protease and helicase activities through the interaction with NS4A. *Biochemistry* 1999;38:5620-32.
21. **Rho J, Choi S, Seong YR, Choi J, Im DS** The arginine-1493 residue in QRRGRTGR1493G motif IV of the hepatitis C virus NS3 helicase domain is essential for NS3 protein methylation by the protein arginine methyltransferase 1. *J Virol* 2001;75:8031-44.

22. **Duong FH, Christen V, Berke JM, Penna SH, Moradpour D, Heim MH** Upregulation of protein phosphatase 2Ac by hepatitis C virus modulates NS3 helicase activity through inhibition of protein arginine methyltransferase 1. *J Virol* 2005;79:15342-50.
23. **Borowski P, Heiland M, Oehlmann K, Becker B, Kornetzky L, Feucht H, Laufs R** Non-structural protein 3 of hepatitis C virus inhibits phosphorylation mediated by cAMP-dependent protein kinase. *Eur J Biochem* 1996;237:611-8.
24. **Borowski P, Schulze zur WJ, Resch K, Feucht H, Laufs R, Schmitz H** Protein kinase C recognizes the protein kinase A-binding motif of nonstructural protein 3 of hepatitis C virus. *J Biol Chem* 1999;274:30722-8.
25. **Ishido S, Hotta H** Complex formation of the nonstructural protein 3 of hepatitis C virus with the p53 tumor suppressor. *FEBS Lett* 1998;438:258-62.
26. **Otsuka M, Kato N, Moriyama M, Taniguchi H, Wang Y, Dharel N, Kawabe T, Omata M** Interaction between the HCV NS3 protein and the host TBK1 protein leads to inhibition of cellular antiviral responses. *Hepatology* 2005;41:1004-12.
27. **Kaul A, Worz I, Bartenschlager R** Adaptation of the hepatitis C virus to cell culture. *Methods Mol Biol* 2009;510:361-72.
28. **Ma Y, Yates J, Liang Y, Lemon SM, Yi M** NS3 helicase domains involved in infectious intracellular hepatitis C virus particle assembly. *J Virol* 2008;82:7624-39.
29. **Krieger N, Lohmann V, Bartenschlager R** Enhancement of hepatitis C virus RNA replication by cell culture-adaptive mutations. *J Virol* 2001;75:4614-24.
30. **Driessen HP, de Jong WW, Tesser GI, Bloemendal H** The mechanism of N-terminal acetylation of proteins. *CRC Crit Rev Biochem* 1985;18:281-325.
31. **Lohmann V, Korner F, Koch J, Herian U, Theilmann L, Bartenschlager R** Replication of subgenomic hepatitis C virus RNAs in a hepatoma cell line. *Science* 1999;285:110-3.
32. **Cohen P** The regulation of protein function by multisite phosphorylation--a 25 year update. *Trends Biochem Sci* 2000;25:596-601.
33. **Yamagata A, Kristensen DB, Takeda Y, Miyamoto Y, Okada K, Inamatsu M, Yoshizato K** Mapping of phosphorylated proteins on two-dimensional polyacrylamide gels using protein phosphatase. *Proteomics* 2002;2:1267-76.
34. **Behnia R, Panic B, Whyte JR, Munro S** Targeting of the Arf-like GTPase Arl3p to the Golgi requires N-terminal acetylation and the membrane protein Sys1p. *Nat Cell Biol* 2004;6:405-13.
35. **Setty SR, Strohlic TI, Tong AH, Boone C, Burd CG** Golgi targeting of ARF-like GTPase Arl3p requires its N-terminal acetylation and the integral membrane protein Sys1p. *Nat Cell Biol* 2004;6:414-9.
36. **Polevoda B, Sherman F** N-terminal acetyltransferases and sequence requirements for N-terminal acetylation of eukaryotic proteins. *J Mol Biol* 2003;325:595-622.
37. **Ogino T, Fukuda H, Imajoh-Ohmi S, Kohara M, Nomoto A** Membrane binding properties and terminal residues of the mature hepatitis C virus capsid protein in insect cells. *J Virol* 2004;78:11766-77.
38. **Tercero JC, Wickner RB** MAK3 encodes an N-acetyltransferase whose modification of the L-A gag NH2 terminus is necessary for virus particle assembly. *J Biol Chem* 1992;267:20277-81.
39. **Yao N, Reichert P, Taremi SS, Prosis WW, Weber PC** Molecular views of viral polyprotein processing revealed by the crystal structure of the hepatitis C virus bifunctional protease-helicase. *Structure* 1999;7:1353-63.
40. **Yi M, Lemon SM** Adaptive mutations producing efficient replication of genotype 1a hepatitis C virus RNA in normal Huh7 cells. *J Virol* 2004;78:7904-15.
41. **Appel N, Pietschmann T, Bartenschlager R** Mutational analysis of hepatitis C virus nonstructural protein 5A: potential role of differential phosphorylation in RNA replication and identification of a genetically flexible domain. *J Virol* 2005;79:3187-94.
42. **Evans MJ, Rice CM, Goff SP** Phosphorylation of hepatitis C virus nonstructural protein 5A modulates its protein interactions and viral RNA replication. *Proc Natl Acad Sci U S A* 2004;101:13038-43.

43. **Masaki T, Suzuki R, Murakami K, Aizaki H, Ishii K, Murayama A, Date T, Matsuura Y, Miyamura T, Wakita T, Suzuki T** Interaction of hepatitis C virus nonstructural protein 5A with core protein is critical for the production of infectious virus particles. *J Virol* 2008;82:7964-76.
44. **Thingholm TE, Jensen ON, Larsen MR** Analytical strategies for phosphoproteomics. *Proteomics* 2009;9:1451-68.
45. **Sarioglu H, Lottspeich F, Walk T, Jung G, Eckerskorn C** Deamidation as a widespread phenomenon in two-dimensional polyacrylamide gel electrophoresis of human blood plasma proteins. *Electrophoresis* 2000;21:2209-18.
46. **Lutter P, Meyer HE, Langer M, Witthohn K, Dormeyer W, Sickmann A, Bluggel M** Investigation of charge variants of rV<sub>iscumin</sub> by two-dimensional gel electrophoresis and mass spectrometry. *Electrophoresis* 2001;22:2888-97.
47. **McBride AE, Silver PA** State of the arg: protein methylation at arginine comes of age. *Cell* 2001;106:5-8.

